Landscape and Urban Planning 102 (2011) 245–253

Contents lists available at ScienceDirect

Landscape and Urban Planning

journal homepage: www.elsevier.com/locate/landurbplan

A study of the "wall effect" caused by proliferation of high-rise buildings using GIS techniques

Man Sing Wong[a], Janet Nichol[a,*], Edward Ng[b]

[a] Department of Land Surveying and Geo-Informatics, The Hong Kong Polytechnic University, Kowloon, Hong Kong
[b] Department of Architecture, The Chinese University of Hong Kong, Hong Kong

ARTICLE INFO

Article history:
Received 19 January 2011
Received in revised form 2 May 2011
Accepted 11 May 2011
Available online 8 June 2011

Keywords:
Frontal area index
Geographic Information Systems
Thermal remote sensing
Ventilation
Wall effect

ABSTRACT

This paper describes a novel method using Geographic Information Systems (GIS) to investigate the "wall effect" caused by proliferation of high-rise buildings along the coast in Kowloon Peninsula of Hong Kong. The research utilises the concept of building frontal area index which is calculated based on three dimensional buildings in 100 m grid cells. The main ventilation pathways across the urban area are located using Least Cost Path analysis in a raster GIS and validated by field measurements. Field measurements were also taken in front of windward and leeward buildings. Results show that winds are forced by high frontal area values, to deviate around coastlines with blocks of "wall effect" buildings parallel to the coast. Average wind speeds of 10.5 m s^{-1} were observed on the windward side of "wall effect" buildings defined according to a southeasterly wind direction, while average wind speeds immediately to the lee side of "wall effect" buildings as well as further inland, were approximately 2.5 m s^{-1} (four times lower). To confirm the "wall effect" hypothesis, scenario analysis was performed by removing these buildings from the model and re-running it. This revealed a 5% increase of air ventilation to urban areas inland, since more fresh onshore air is able to penetrate from the coast. This improvement is significant since only 0.05% of buildings in the study area were removed. Overlay of the ventilation pathways over a thermal satellite image representing Heat Island Intensity (HII) indicated significantly lower HII values, and reduced extent of the core HII areas, around the ventilation paths.

1. Introduction

In affluent coastal cities with high land prices, unrestricted commercial exploitation of land commonly gives rise to a distinctive pattern of building development, known in Hong Kong as the "wall effect". This term aptly describes a coastline with high-rise buildings oriented parallel to the coast in order to maximise sea views and developers' profits. At the same time, adjacent buildings and those farther inland suffer from blocked views, lower sunshine and light levels, and well as the build-up of pollution and an urban heat island effect due to lack of ventilation. The term "wall effect" thus has negative connotations, and has become a controversial issue in Hong Kong, where the lack of flat land has given rise to extremely high built densities, which in turn generate an urban heat island of up to 12 °C in the urban core (Nichol, 2005; Nichol, Fung, Lam, & Wong, 2009). The general characteristics of "wall effect" have been defined as (i) less than 15 m between the frontal (blocking) buildings and those behind, (ii) frontal buildings are taller than those behind, (iii) frontal buildings have more than 35 floors and (iv) frontal buildings face the prevailing wind (Yim, Fung, Lau, & Kot, 2009).

As urban populations increase, many modern cities in both temperate (Baker et al., 2003; Hawkins, Brazel, Stefanov, Bigler, & Saffell, 2004; Oke, 1982) and tropical regions (Fung, Lam, Nichol, & Wong, 2009; González, Luvall, Rickman, Comarazamy, & Picón, 2007; Jusuf, Wong, Hagen, Anggoro, & Hong, 2007; Nichol, 1996, 2005; Nichol et al., 2009) are reporting significant heat island effects resulting from high building densities. Air flow between rural and urban areas is one of the parameters governing urban heat island formation and the build-up of pollution (Haeger-Eugensson & Holmer, 1999; Oke, 1982). The core of Hong Kong's urban heat island is the mixed commercial and residential district of Mongkok (Fung et al., 2009; Nichol et al., 2009), the world's most densely populated urban district, which is situated in the middle of the urbanised Kowloon Peninsula, approximately 2 km from the coast. Mongkok and other inner districts also suffer from air pollution levels several times higher than air quality standards for the basic pollutants (Louie et al., 2005), e.g. the annual U.S. Environmental Protection Agency standard for $PM_{2.5}$ (particulate matter with diameter of 2.5 μm or less) is 15 μg m^{-3}, and all five of Hong Kong's

* Corresponding author. Tel.: +852 27665952; fax: +852 23302994.
E-mail addresses: m.wong06@fulbrightmail.org (M.S. Wong), lsjanet@inet.polyu.edu.hk, lsjanet@polyu.edu.hk (J. Nichol), edwardng@cuhk.edu.hk (E. Ng).

0169-2046/$ – see front matter © 2011 Elsevier B.V. All rights reserved.
doi:10.1016/j.landurbplan.2011.05.003

$PM_{2.5}$ monitoring stations recorded more than double this amount for every year from 2003 to 2007 (EPD, 2009). The controversy surrounding the "wall effect" has led to the need to evaluate its impacts on urban temperature and air quality due to the blocking of sea breezes and reduced ventilation to inner areas. Yim et al. (2009) conducted the only previous study of the ventilation impacts of "wall effect" buildings on the adjacent street environment using a Computational Fluid Dynamics (CFD) model. In their study, the modelling results were validated by a wind tunnel simulation. The results predicted that the air velocity at 2 m above the ground in a street canyon would decrease by approximately 30% and 40%, if wall buildings upwind are 2 times or 4 times the height of the street canyon respectively and the retention time of pollutants would increase by 45% and 80%.

Such CFD models are widely used for flow analysis around fixed structures in engineering and urban planning (Baik & Kim, 1999), and prediction of air pollution dispersal (Blocken, Carmeliet, & Stathopoulos, 2007; Huber et al., 2004; Kondo, Asahi, Tomizuka, & Suzuki, 2006). They depend on reconstructing the real urban geometry of a particular city to simulate air flow at building and street level. The computer-intensive nature of CFD models precludes their application to large areas or whole cities, but they can represent highly detailed flow patterns for small areas. An alternative approach for reconstruction of wind flow patterns and pollution dispersal at large scales over a district is the wind tunnel model. For example, Duijm (1996) used an atmospheric boundary layer wind tunnel in Lantau island, Hong Kong at the large scale of 1:4000 over a small rural study area, and Mfula, Kukadia, Griffiths, and Hall (2005) used a wind tunnel at a nominal building scale of 1:100 to determine the pollution source regions for buildings. Although the wind tunnel model can accurately represent urban ventilation under constrained conditions, like the CFD model, the small area covered, as well as high computer demands and operating costs discourage their use. Recently, several numerical models have been developed for modelling air flow over larger areas but at coarser resolution, including the Pennsylvania State University/National Center for Atmospheric Research (PSU/NCAR) mesoscale model (the Fifth-Generation Mesoscale Model, known as MM5). The MM5 model operates at mesoscale, to simulate phenomena such as mountain-valley and land-sea breezes (Dudhia, Gill, Manning, Wang, & Bruyere, 2003). Although Yim et al.'s (2009) study provides a method for the detailed depiction of the "wall effect" on a street canyon in Hong Kong, the model is limited to small areas, whereas the blocking of sea breezes as well as prevailing winds by tall buildings is likely to have wider impacts at district and city level. Thus application of wind ventilation models derived at detailed (street) level to whole city (city-scale), especially in dense urban regions with complex street and building structures is challenging.

The now ready availability of three dimensional digital data of modern cities on a Geographic Information Systems (GIS) platform enables the estimation of roughness parameters for wind ventilation modelling. The roughness parameters are zero-plane displacement height (z_d) and roughness length (z_0) (Counihan, 1975; Lettau, 1969), plan area density (λ_p), frontal area index (λ_f) (Burian, Brown, & Linger, 2002; Grimmond & Oke, 1999), average height weighted with frontal area (z_h), depth of the roughness sub-layer (z_r) (Bottema, 1997; Grimmond & Oke, 1999) and the effective height (h_{eff}) (Matzarakis & Mayer, 1992). The concept of frontal area index (λ_f) was introduced by Grimmond and Oke (1999) to represent the aerodynamic properties or roughness of the urban surface in mesoscale modelling of the urban climate. The λ_f is obtained from the surface area of all vertical building walls facing wind flow in a particular direction (frontal area per unit horizontal area) (Fig. 1). The frontal area index has a strong relationship with the roughness of the urban surface, and it influences the flow regime within urban street canyons (Burian et al., 2002).

For wind ventilation depiction, Gál and Unger (2009) proposed to inspect visually the ventilation paths depicted by frontal area index data. Although this method is feasible for a small study area, it cannot work across a whole city and the results cannot be validated quantitatively. Therefore, for transforming the frontal area index (pixel-base) to air corridor (path-base), least cost path analysis can be conducted on a GIS platform. This simulates the fresh air corridors based on the least resistance of λ_f across a city, e.g. high connectivity along the least cost path represents corridors of strong wind ventilation.

The aims of this paper are (i) to investigate the "wall effect" created by buildings along the coastline in Hong Kong using frontal area index values and least cost path analysis and (ii) to quantify the impacts of the "wall effect" on air flow across the city.

2. Study area

The study area is the highly urbanised 160 km^2 Kowloon Peninsula of Hong Kong, which has a mean population density of 43,000 persons/km^2, and the highest population density in the world (130,000 persons/km^2) in Mongkok district. The topography is mainly flat, but rises to 300 m at the northern edge, and one large park (Kowloon park) and a few small urban parks of less than 1 ha each, separate the generally built-up landscape. The climate is sub-tropical, with hot humid summers, and there is a marked urban heat island due to the high density and high rise urban form (Wong, Nichol, & Lee, 2010). Since Kowloon is a peninsula with few locations over 3 km from the coast, there is a strong belief by residents that the main cause of the urban heat island is the "wall effect", which prevents cool sea breezes from penetrating to the inner city. The environmental group Green Sense surveyed 155 housing estates in Kowloon and found that 104 of these have a "wall-like" design (Green Sense, 2009).

3. Frontal area index

The frontal area index (λ_f) is calculated as the total area of building facets projected to plane normal facing the particular wind direction, divided by the plane area (Burian et al., 2002; Grimmond & Oke, 1999; Wong, Nichol, To, & Wang, 2010) (Eq. (1), Fig. 1).

$$\mathrm{FAI} = \frac{\mathrm{Area}_{\mathrm{facets}} \cdot Z_{\mathrm{mean\ plane}}}{\mathrm{Area}_{\mathrm{plane}}} \quad (1)$$

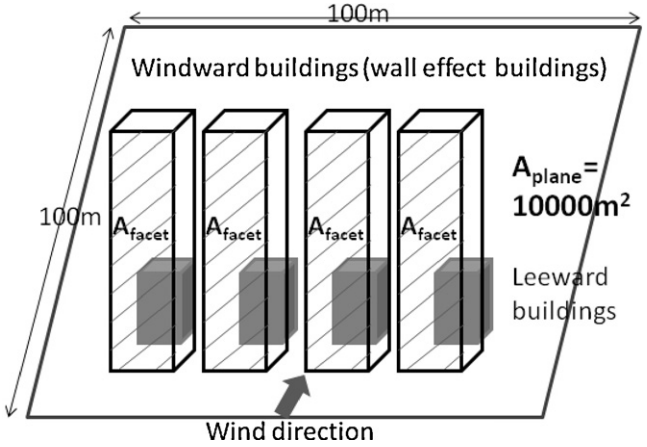

Fig. 1. Example of frontal area calculation.

where FAI is the frontal area index, $Area_{facets}$ is the total area of building facets facing the wind direction, $Area_{plane}$ is the plane area and $Z_{mean\ plane}$ is the mean height of plane area.

In this study, digital data of building polygons at 1:5000 scale were obtained from the Hong Kong Lands Department. A program was written in ESRI® ArcGIS™ 9.2 software to estimate the total frontal area in the projected plane normal to the specific wind direction (Wong, Nichol, To, et al., 2010). The calculated frontal areas are stored on horizontal plane polygons (e.g. grid cells of 100 m × 100 m, being the resolution selected for this study). In this study, λ_f at 100 m resolution over the whole of Kowloon Peninsula (approximate 11 km by 7 km) was calculated for eight different wind directions (north, northeast, east, southeast, south, southwest, west, and northwest).

As shown in Fig. 2, an average value of $\lambda_f = 0.3$ is observed over the whole study area, with somewhat higher λ_f values near the west coast of the peninsula. Burian et al. (2002) found that the λ_f in residential, commercial and industrial districts in Los Angeles, were 0.176, 0.246, and 0.095 respectively but since their methods of calculating λ_f included the frontal areas for every facet including both windward and leeward buildings, direct comparison with our study cannot be made.

4. Least cost path analysis

The rationale of least cost path (LCP) analysis is to calculate a path between a starting and ending point with the least cost to traverse. The cost can be quantified as a function of time (e.g. shortest time), distance (e.g. shortest path), or by user-defined criteria. It is applicable in habitat and ecological modelling, landscape and network analysis, pollutant dispersion modelling and traffic analysis. In this study, the LCP was used to permit the designation of pathways across a city following paths of least resistance through streets and buildings, based on the frontal area index map. Thus, the LCP procedure uses maps of frontal area index to designate routes with a high probability of strong ventilation as well as a high degree of connectivity between starting and ending points. The LCP module in IDRISI v.14.02 (Clark Labs., Worcester, MA, USA) was customised to calculate the degree of wind obstruction (λ_f) and thus to map potential ventilation routes (Wong, Nichol, To, et al., 2010). Thirty six starting points were spaced evenly, offshore of the east coast of the Kowloon Peninsula, to represent easterly wind movement across the peninsula towards the west (Fig. 3). A total of 1296 LCPs represent easterly winds from many combinations of starting and ending points. A large number of routes were thus superimposed on each other in many places, and the occurrence frequencies for each 100 m grid cell were calculated, by counting the number of overlaid routes passing through the cell. It is assumed that cells with high occurrence frequencies have stronger air flow and better ventilation than those with few, or no paths through them.

Routes with the highest frequency of LCPs (over 100 occurrences in each grid cell along the route) are shown in Fig. 3a, which represents easterly wind ventilation paths. These paths are located on:

i. *Path A*: This route traverses the old Kai Tak airport (open abandoned land), low-rise residential areas along Boundary Street and reaches Nam Cheong Park on the west coast. The occurrence frequency in grid cells along this route comprises more than 11% of the total, i.e., average of 150 occurrences per cell along the route out of the total of 1296 routes generated.
ii. *Path B*: This is the shortest route, but corresponds to a four-lane wide dual-carriageway (Waterloo street) connecting the old airport on the east coast to the west coast. This route constitutes a strategic fresh air ventilation pathway from east to west across the most congested part of the city since it bisects the most densely built district of Mongkok and reaches the west Kowloon cultural district (reclaimed land designated for development). The occurrence frequency of pathways in grid cells along this route is above 13% (i.e. 170/1296).
iii. *Path C*: Hong Chong road, Cheong Wan road, Austin road, Kowloon Cricket club, Gascoigne road, west Kowloon cultural district (P_c in Fig. 3a). This route traverses a university, low

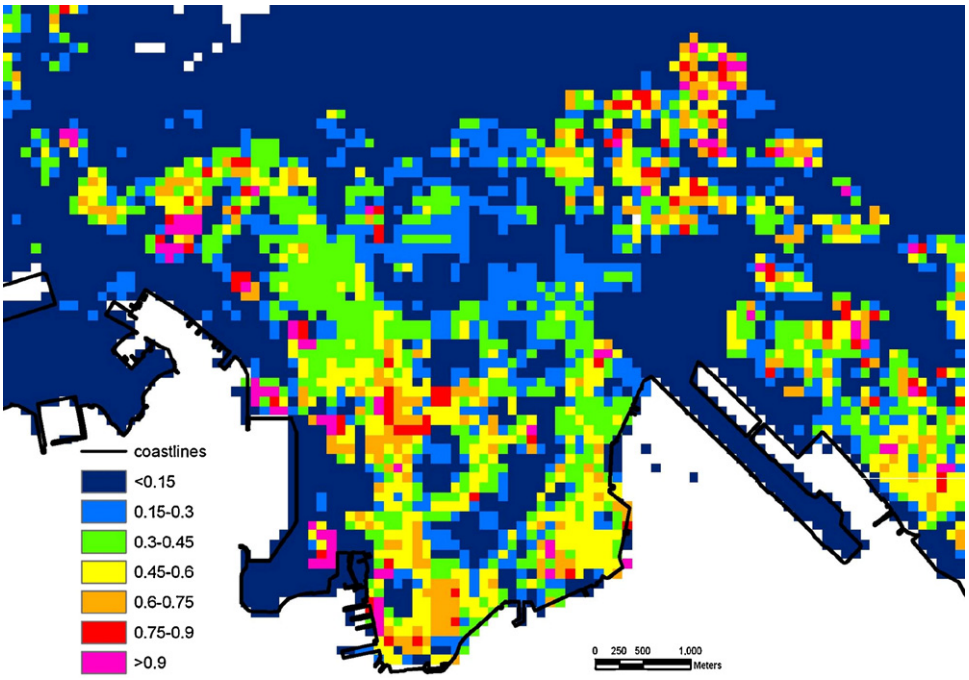

Fig. 2. Frontal area index map, blue colour represents very low frontal area index (i.e. wind is not blocked by any building), magenta colour represents very high frontal area index (i.e. wind is mostly blocked by buildings). (For interpretation of the references to colour in this figure legend, the reader is referred to the web version of the article.)

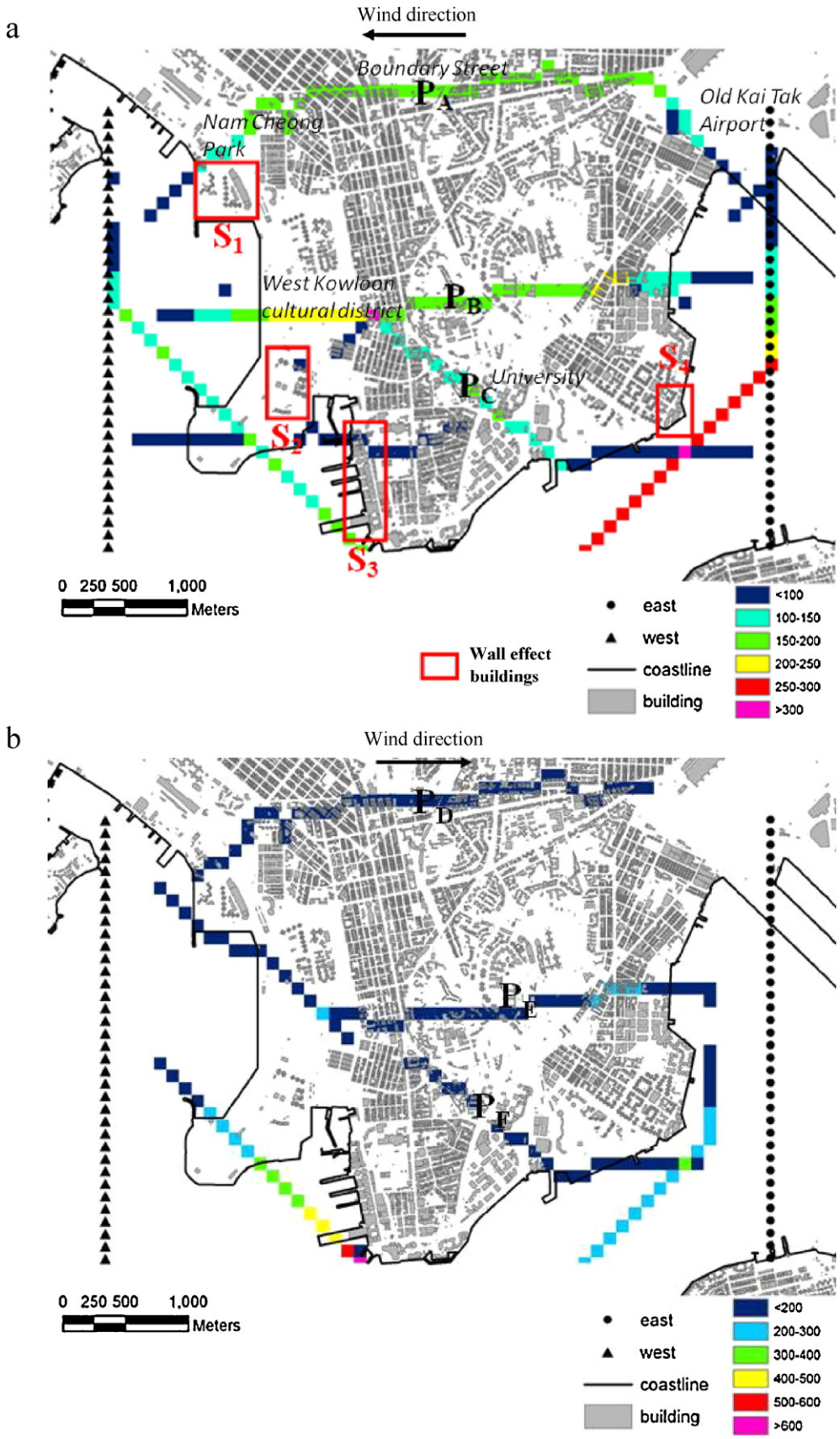

Fig. 3. Occurrence frequency of ventilation paths in (a) east–west direction (total number of paths is 1296); (b) west–east direction (total number of paths is 1296).

density treed residential area, and densely built commercial districts. The occurrence frequency in grid cells along this route is ca. 11% (i.e. 140/1296) which is the lowest frequency among the three main paths.

These three paths with wind flow from east to west have occurrence frequencies of 11% or more. The three main westerly paths (Fig. 3b) (with between 14% and 19% occurrence frequency) are described below:

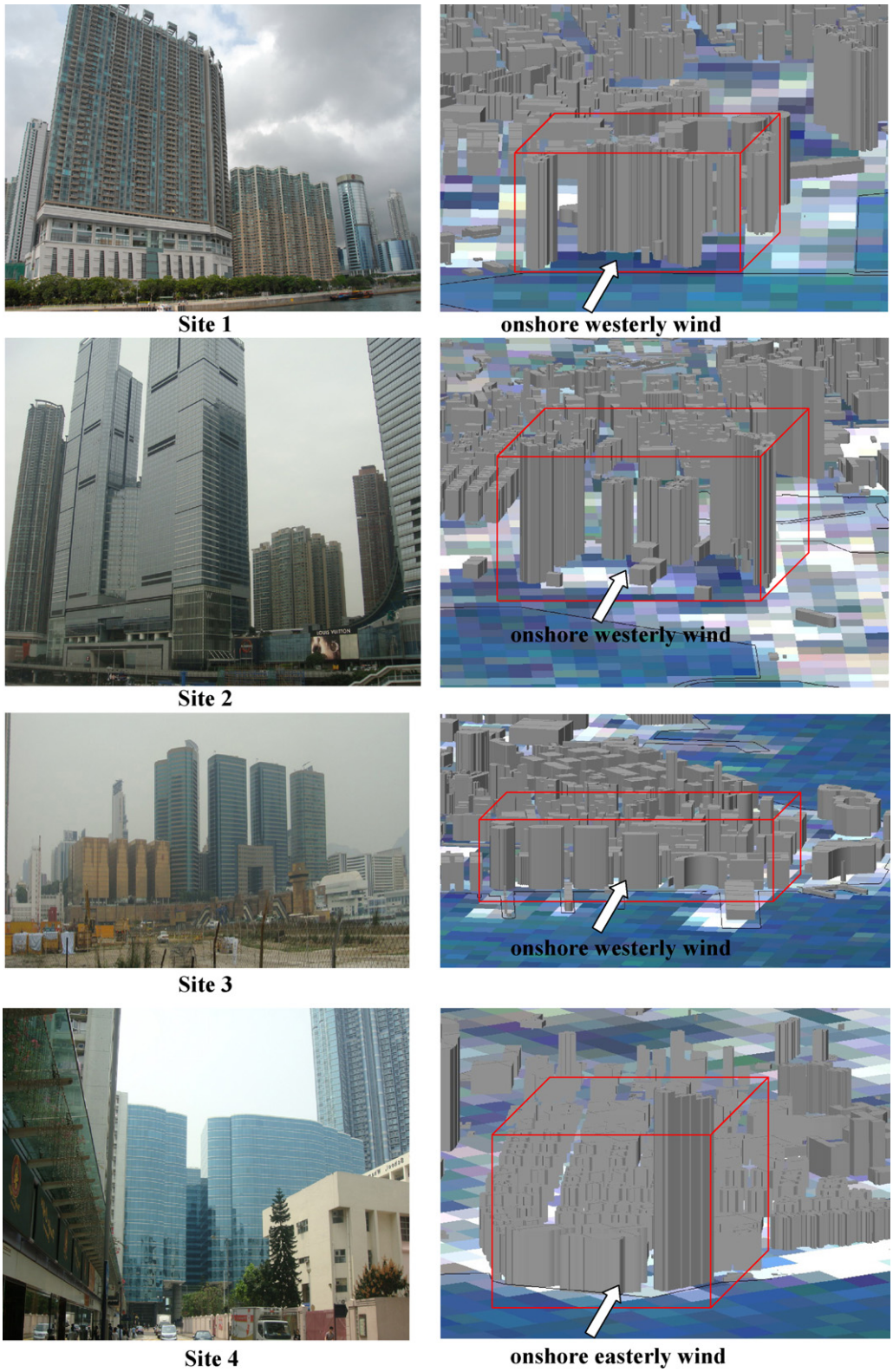

Fig. 4. 3D models of "wall effect" buildings and site inspection photos (Fig. 4d is taken from landward direction).

iv. *Path D*: Similar to Path A, but the occurrence frequency in grid cells along this route comprises more than 14% of the total (180 out of 1296 paths).
v. *Path E*: Similar to Path B, but this route traverses southeasterly along Lin Cheung road and Lai Cheung road initially, then joins the latter part of B. The occurrence frequency in grid cells along this route comprises more than 15% of the total (200 out of 1296 paths).
vi. *Path F*: Similar to Path C, but this route traverses southeasterly along Lin Cheung road and Lai Cheung road initially, then joins the latter part of B. This route is represented by occurrence frequency greater than 19% (250 out of 1296 paths).

These six generated pathways were considered to have a high probability of stronger and more frequent air movement than other areas. The shift angles (inclination of the wind paths) of these six pathways are generally less than 30° except Path A (ca. 40°), which shows good continuation of air path in aerodynamic aspect.

The high-rise buildings parallel to the coast are designated by red boxes, namely S_1 (Olympic City), S_2 (Union Square), S_3 (Harbor city), S_4 (Harbor Plaza). It can be seen that the paths are constrained by high λ_f values and have to deviate around the two coastlines with major "wall effect" buildings. Since these buildings at S_1, S_2, and S_3 have been built to maximise sea views, with their longest facets parallel to the coastline, they face and thus interrupt the westerly and southwesterly, onshore sea breezes which occur mostly in summer. These buildings at S_4 face directly into the easterly wind which is the prevailing wind direction. Fig. 4 shows the site inspection photos and three dimensional GIS models of the four major groups of "wall effect" buildings in the Kowloon Peninsula. A comparison between these "wall effect" buildings with a Heat Island Intensity (HII) map derived from a thermal satellite image was made. HII is a more objective and absolute measure of heat island magnitude, and it represents the difference in air temperatures between city center and rural areas. For this study, the HII values were derived from an ASTER thermal satellite image, which was regressed against extensive ground level air temperature data collected at the image time (Fung et al., 2009). The thermal image resolution was enhanced to 10 m using emissivity modulation technique (Nichol, 2009). The results indicate that the highest HII values are immediately, as well as more generally, inland of these densely built coastlines (Fig. 5), i.e. higher HII values ($\geq$7 °C) represent heat island core areas. These have become heat island core areas (red and purple areas), and include Mongkok inland of S_1 and Hung Hom inland of S_4, but do not include Tsim Sha Tsui S_3 which has an urban park on the lee side of the "wall effect" coast. Fig. 5 shows the designated ventilation paths overlaid onto the HII image. All three paths (Paths D, E, and F) cross these heat island core areas (magenta colour) at the shortest distance, e.g. Path E, crosses the region of greatest heat island intensity at Yau Ma Tei (For interpretation of the references to colour in this figure legend, the reader is referred to the web version of the article.). The relationships between λ_f and HII were analysed at pixel scale (i.e. 100 m) as well as at regional scale (i.e. for 68 Tertiary Planning Units—which represent basic socioeconomic units for planning purposes). The correlation at regional scale is significantly higher (r = 0.780) than that at pixel scale (r = 0.492), but both are significant at the 1% confidence level.

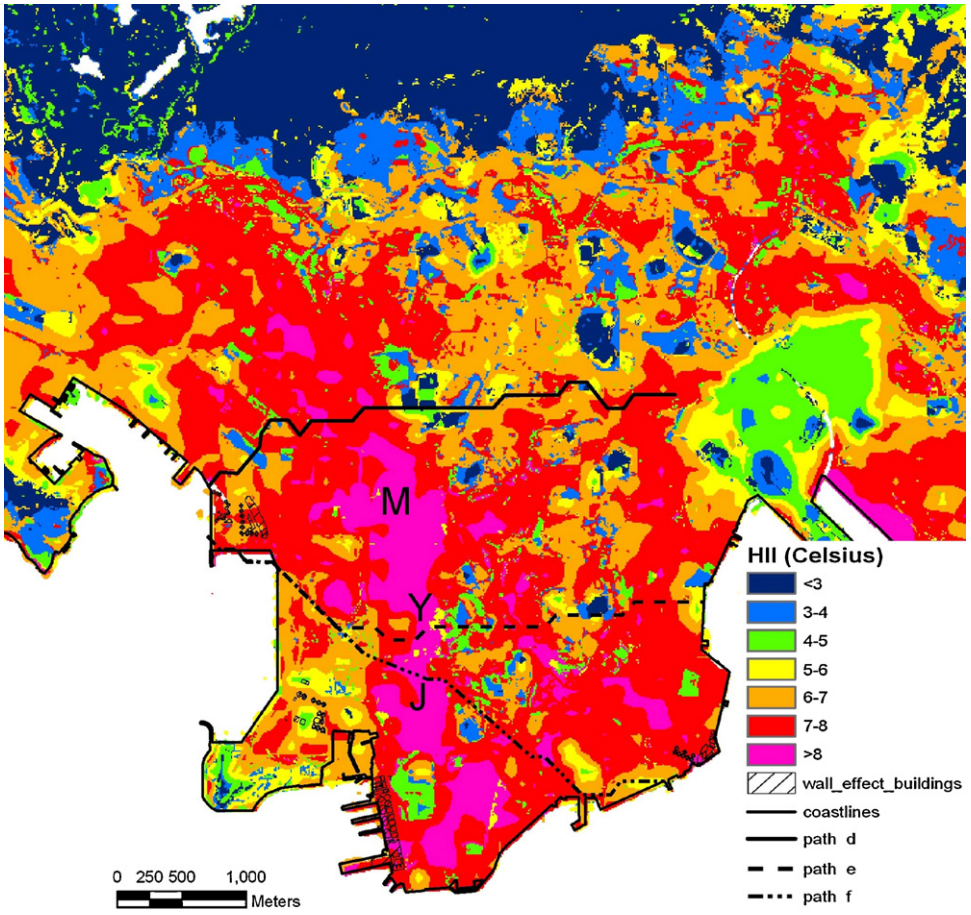

Fig. 5. Designated ventilation paths in west–east direction and "wall effect" buildings overlaid on heat island intensity image derived from a nighttime ASTER thermal (10.25–10.95 μm) image on 31 January 2007 at 10 m resolution, Label M, Y and J represent Mongkok, Yau Ma Tei and Jordan respectively.

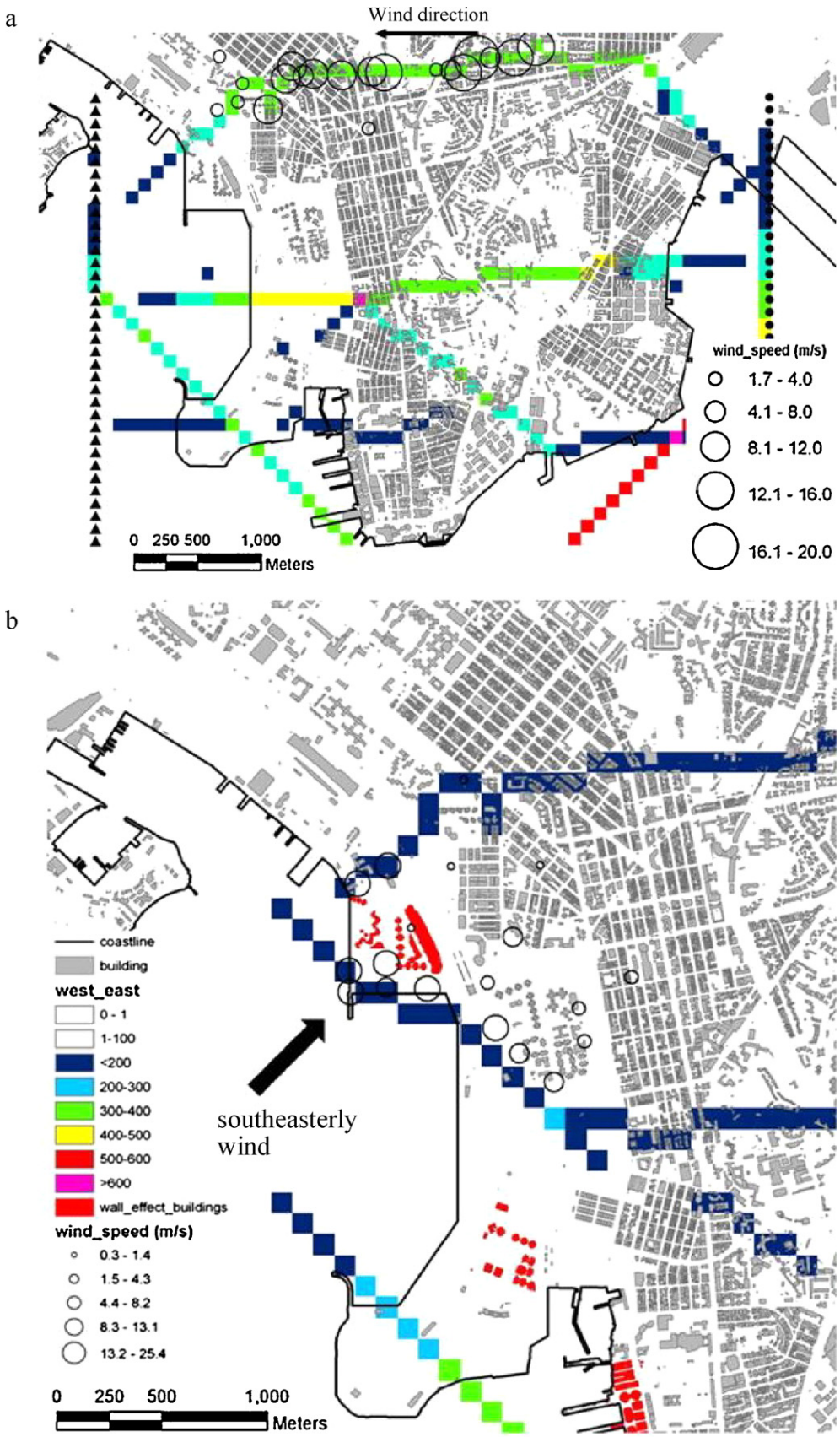

Fig. 6. (a) Occurrence frequency of ventilation paths overlaid with field measurements in east-west direction; (b) wind speed measurements on site 1 (Olympic City), in front of windward and leeward buildings.

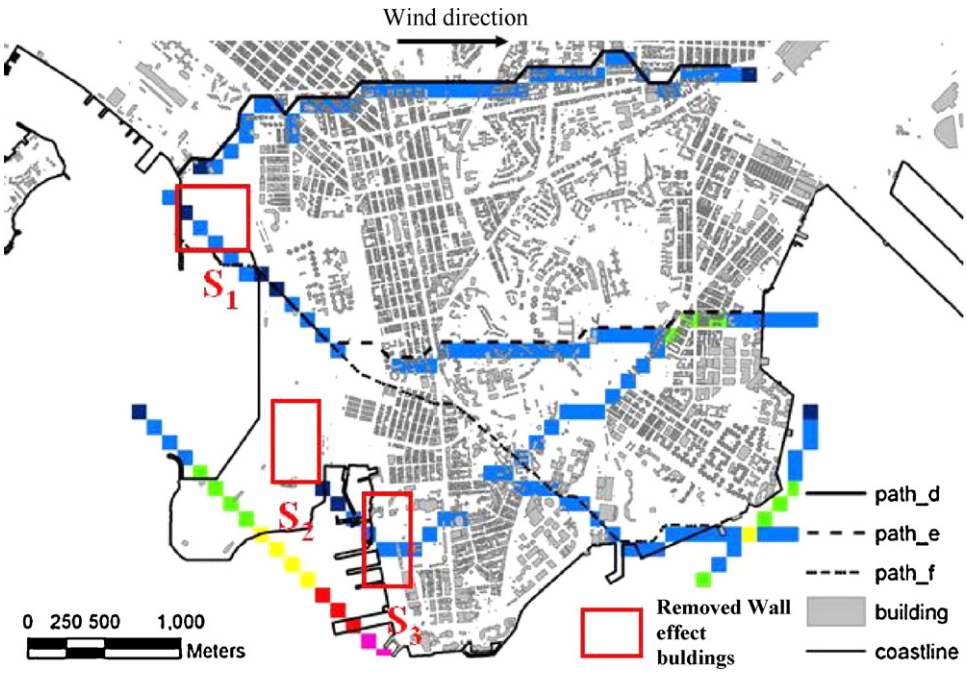

Fig. 7. Occurrence frequency of ventilation paths (removed the "wall effect" buildings—in red colour) in west–east direction. Colour legend as for Fig. 6b. (For interpretation of the references to color in this figure legend, the reader is referred to the web version of the article.)

5. Validation strategy

The significance and functionality of the mapped ventilation paths was verified by fieldwork carried out on 13 October 2009, 14 April 2010, 30 May 2010, 5 July 2010, 14 July 2010, 27 July 2010. These dates represent the easterly wind dominant throughout the year, and the southwesterly sea breezes in the warmer parts of the year. First, a slow walk was undertaken along the Path A, recording the wind speed and GPS locations. Wind speeds were measured 4 times at each point along the paths, resulting in 132 readings from Path A, and the results were averaged. Only Path A was validated, since it is deemed to be a key corridor for both easterly and westerly winds (Path A is exactly the same as Path D: the only common path for both easterly and westerly winds). The field measurements located on the ventilation paths are shown in Fig. 6, and the dot sizes represent wind speeds at those locations along the path. Along Path A, average and maximum wind speeds of 9.3 m s^{-1} and 17.8 m s^{-1} were observed respectively. However, wind speeds at locations off the path were much lower (ca. 2.3 m s^{-1}), and more similar to the wind speed of 2 m s^{-1} recorded by the Mongkok climate station at the time. About 55% of the field readings with wind speed above 9.1 m s^{-1} fall in Path A (with 24% of all paths generated). Thus Path A appears to be a key fresh air corridor for air flow in the dominant wind direction from east to west across the Kowloon Peninsula. Secondly, the impacts of the "wall effect" on air flow were quantified by the measurement of wind speeds to the windward and leeward of "wall effect" buildings facing the southeasterly winds at site 1 (Olympic city). Average and maximum wind speeds of 10.5 m s^{-1} and 13.1 m s^{-1} were observed to the windward of the buildings. However, average wind speed leeward of the "wall effect" buildings and in inner areas was four times lower (~2.5 m s^{-1}). Our observations show that windspeeds decrease by ca. 76% between the windward and leeward sides of the buildings, suggesting a significant impact on urban ventilation.

6. Scenario analysis

In Fig. 7, the "wall effect" buildings have been removed (S_1, S_2, S_3, S_4, red colour in Fig. 7), the λ_f and the LCPs were re-generated for the westerly wind direction, as most of the "wall effect" buildings are along on the west coast. The distribution of path frequencies for Path D gave somewhat similar results between hypothetical and real situations, but Path D in the hypothesis map shifted several pixels inland. Removal of the "wall effect" buildings also permits a new path to be identified between S_2 and S_3, which provides fresh onshore air to the densely-built shopping and residential district of Tsim Sha Tsui. Another improvement is an additional major ventilation pathway running across the Kowloon Peninsula from the region of "wall effect" buildings at S_2 and S_3 in the southwest, towards the northeast. This path would be capable of mitigating heat island effects in the densest commercial–residential districts of Jordan and Yau Ma Tei. This new path shown in Fig. 7 has high occurrence frequency, representing 21% of the overall westerly wind flow, compared with only 16% previously, since due to the "wall effect", a significant proportion of the overall wind flow is deflected away from the urban area. Thus it appears the removal of "wall effect" buildings can improve the ventilation in this inner district by 5%, since the original paths across this district accounted for an average of only 16% of the overall westerly wind flow. The magnitude is significant and it is expected that the improvement of air ventilation by removal of key "wall effect" buildings would also have a significant impact on heat island build-up in inner areas.

7. Conclusion

This paper investigates the impact of "wall effect" buildings on air ventilation within densely built districts using frontal area index and least cost path analysis models. When all LCP paths are overlaid to derive maps of pathways with a high probability of stronger and more frequent air movement, three paths (Paths A, B, and C) accounted for 11%, 13%, 11% frequency respectively of all easterly wind flow, and Paths D, E, and F accounted for 14%, 15%, 19% frequency respectively of the all westerly wind flow. Therefore, these paths, out of a total of 1296 paths, account for as much as 35% and 48% of the total wind from easterly and westerly directions across the urban area. When wind speeds were measured in the field to

evaluate the relevance of the models, they compared well with the frequencies of the modelled pathways.

It was found that most of the paths especially Path E cross the heat island core areas at the shortest distances, and since the ventilation paths have been validated by field work this provides strong evidence that the paths acts as fresh air corridors, reducing the extent of the heat island core areas as well as the magnitude of HII. The correlations between HII and frontal area index ($r = 0.780$ and $r = 0.492$ at regional and pixel level respectively) are slightly higher than the correlations between both building density and frontal area index, and building height and frontal area index, i.e. $r = 0.603$, $r = 0.527$ at regional level respectively (Wong, Nichol, To, et al., 2010). This suggests that the frontal area index is a more useful parameter than either building density or building height in heat island analysis, probably because it is a holistic parameter which represents both the density and height of buildings in a particular area. Therefore it can be used as a single parameter in planning assessments for heat island mitigation. Future improvements to the model may include finding the approximate optimal resolutions for HII and frontal area index. In such a densely urbanised and populated study area, the wide ventilation corridors of 100 m width used in this study may not appear to provide viable connecting corridors at street scale, since most urban canyons are much narrower, although a 100 m grid is sufficient for city scale modelling. However, the model of frontal area index can be adapted for any grid resolution depending on the morphology of any particular city.

To evaluate the impact of "wall effect" buildings in the study area, wind speeds on site 1 (Olympic City) were measured both windward and leeward of "wall effect" buildings. Results showed that an average wind speed of 10.5 m s^{-1} was observed to windward of "wall effect" buildings facing southeasterly winds, and average wind speeds behind these buildings were four times lower ($\sim$2.5 m s^{-1}). When scenario analysis was carried out by removing four groups of "wall effect" buildings (a total of 101 buildings removed, or 0.05% of the buildings across the whole study area), a significant improvement of 5% increased ventilation over the urban area was generally observed, as represented by additional new paths traversing the urban area. Future improvement in urban ventilation for mitigation of pollution and the urban heat island can be effected by more strategic placement of high-rise buildings in coastal and near-coastal locations.

This study offers a simple and low cost method to investigate the impact of "wall effect" buildings on air ventilation over a city at detailed level. City planners and environmental authorities may use the derived models for pinpointing the key buildings which impede air flow to the urban core.

Acknowledgments

The authors would like to acknowledge the Hong Kong Planning Department for land use and Tertiary Planning Unit data and the Lands Department for building GIS databases. This project was funded by Public Policy Research Project PPR-K-QZ04 and PolyU FCLU Sustainable Urbanisation Research Fund (SURF) (1-ZV4V).

References

Baik, J. J., & Kim, J. J. (1999). A numerical study of flow and pollutant dispersion characteristics in urban street canyons. *Journal of Applied Meteorology*, *38*, 1576–1589.

Baker, L., Brazel, A., Selover, N., Martin, C., McIntyre, N., Steiner, F., et al. (2003). Urbanization and warming of Phoenix (Arizona, USA): Impacts, feedbacks and mitigation. *Urban Ecosystems*, *6*, 183–203.

Blocken, B., Carmeliet, J., & Stathopoulos, T. (2007). CFD evaluation of the wind speed conditions in passages between buildings—Effect of wall-function roughness modifications on the atmospheric boundary layer flow. *Journal of Wind Engineering and Industrial Aerodynamics*, *95*(9–11), 941–962.

Bottema, M. (1997). Urban roughness modelling in relation to pollutant dispersion. *Atmospheric Environment*, *31*, 3059–3075.

Burian, S. J., Brown, M. J., & Linger, S. P. (2002). *Morphological analysis using 3D building databases* (pp. 36–42). Los Angeles, CA: Los Alamos National Laboratory. [LA-UR-02-0781].

Counihan, J. (1975). Adiabatic atmospheric boundary layers: A review and analysis of data from the period 1880–1972. *Atmospheric Environment*, *9*, 871–905.

Dudhia, J., Gill, D., Manning, K., Wang, W., & Bruyere, C. (2003). *PSU/NCAR mesoscale modeling system tutorial class notes and user's guide. MM5 modeling system version 3*. NCAR.

Duijm, N. J. (1996). Dispersion over complex terrain: Wind-tunnel modelling and analysis techniques. *Atmospheric Environment*, *30*(16), 2839–2852.

EPD. (2009). The Hong Kong Environmental Protection Department, Past Air Pollution Index Record. Environmental Protection Department, Hong Kong. Available from http://www.epd-asg.gov.hk/english/pastapi/pastapie.php Accessed 26.04.10.

Fung, W. Y., Lam, K. S., Nichol, J. E., & Wong, M. S. (2009). Heat island study—Satellite derived air temperature. *Journal of Climate and Applied Meteorology*, *48*(4), 863–872.

Gál, T., & Unger, J. (2009). Detection of ventilation paths using high-resolution roughness parameter mapping in a large urban area. *Building and Environment*, *44*, 198–206.

González, J. E., Luvall, J. C., Rickman, D. L., Comarazamy, D., & Picón, A. J. (2007). Urban heat island identification and climatological analysis in a coastal, tropical city: San Juan, Puerto Rico. In Q. Weng, & D. A. Quattrochi (Eds.), *Urban remote sensing* (pp. 223–252). Florida: CRC Press.

Green Sense. (2009). Environmental Group Green Sense. <http://greensense.org.hk/> Accessed 26.04.10.

Grimmond, C. S. B., & Oke, T. R. (1999). Aerodynamic properties of urban areas derived from analysis of surface form. *Journal of Applied Meteorology*, *34*, 1262–1292.

Haeger-Eugensson, M., & Holmer, B. (1999). Advection caused by the urban heat island circulation as a regulating factor on the nocturnal urban heat island. *International Journal of Climatology*, *19*, 975–988.

Hawkins, T., Brazel, A., Stefanov, W., Bigler, W., & Saffell, E. (2004). The role of rural variability in urban heat island determination for Phoenix, Arizona. *Journal of Applied Meteorology*, *43*(3), 476–486.

Huber, A. H., Tang, W., Flowe, A., Bell, B., Kuehlert, K., & Schwarz, W. (2004). Development and applications of CFD simulations in support of air quality studies involving buildings. In *Proceedings of 13th joint conference on the applications of air pollution meteorology with the Air & Waste Management Association* Vancouver, British Columbia, Canada, August 23–27,

Jusuf, S. K., Wong, N. H., Hagen, E., Anggoro, R., & Hong, Y. (2007). The influence of land use on the urban heat island in Singapore. *Habitat International*, *31*, 232–242.

Kondo, H., Asahi, K., Tomizuka, T., & Suzuki, M. (2006). Numerical analysis of diffusion around a suspended expressway by a multi-scale CFD model. *Atmospheric Environment*, *40*, 2852–2859.

Lettau, H. (1969). Note on aerodynamic roughness-parameter estimation on the basis of roughness-element description. *Journal of Applied Meteorology*, *8*, 828–832.

Louie, P. K. K., Chow, J. C., Chen, L. W., Watson, J. G., Leung, G., & Sin, D. W. M. (2005). PM2.5 chemical composition in Hong Kong: Urban and regional variations. *Science of the Total Environment*, *338*(3), 267–281.

Matzarakis, A., & Mayer, H. (1992). (pp. 13–22). *Mapping of urban air paths for planning in Munchen* Wissenschaftlichte Berichte Institut for Meteorologie und Klimaforschung, The University of Karlsruhe.

Mfula, A. M., Kukadia, V., Griffiths, R. F., & Hall, D. J. (2005). Wind tunnel modelling of urban building exposure to outdoor pollution. *Atmospheric Environment*, *39*(15), 2737–2745.

Nichol, J. E. (1996). High resolution surface temperature patterns related to urban morphology in a tropical city: A satellite-based study. *Journal of Applied Meteorology*, *35*, 135–146.

Nichol, J. E. (2005). Remote sensing of urban heat islands by day and night. *Photogrammetric Engineering and Remote Sensing*, *71*(5), 613–621.

Nichol, J. E. (2009). An emissivity modulation method for spatial enhancement of thermal satellite images in urban heat island analysis. *Photogrammetric Engineering and Remote Sensing*, *75*(5), 547–556.

Nichol, J. E., Fung, W. Y., Lam, K. S., & Wong, M. S. (2009). Urban heat island diagnosis using ASTER satellite images and 'in situ' air temperature. *Atmospheric Research*, *94*(2), 276–284.

Oke, T. R. (1982). The energetic basis of the urban heat island. *Quarterly Journal of the Royal Meteorological Society*, *108*, 1–24.

Wong, M. S., Nichol, J. E., & Lee, K. H. (2010). A satellite view of urban heat island: Causative factors and scenario analysis. *Korean Journal of Remote Sensing*, *26*(6), 617–627.

Wong, M. S., Nichol, J. E., To, P. H., & Wang, J. Z. (2010). A simple method for designation of urban ventilation corridors and its application to urban heat island analysis. *Building and Environment*, *45*(8), 1880–1889.

Yim, S. H. L., Fung, J. C. H., Lau, A. K. H., & Kot, S. C. (2009). Air ventilation impacts of the "wall effect" resulting from the alignment of high-rise buildings. *Atmospheric Environment*, *43*, 4982–4994.